Journal of Applied Polymer Science

Preparation and characterization of PVA membrane modified by water-soluble hyperbranched polyester (WHBP) for the dehydration of *n*-butanol

Qian-Zhi Zhang,[1] Bing-Bing Li,[1] De Sun,[1] Li-Jun Zhang,[1] Da-Yong Li,[2] Ping Yang[1]

[1]Department of Chemical Engineering, Changchun University of Technology, 2055 Yanan Street, Changchun 130012, People's Republic of China

[2]COFCO Bio-Chemical Energy (Yushu) Co. Ltd., Economic Development Wukeshu, 1 Dongfeng Street, Changchun 130033, People's Republic of China

Correspondence to: B.-B. Li (E-mail: libingbing2015@126.com)

ABSTRACT: Water-soluble hyperbranched polyester (WHBP) was synthesized through the esterification reaction of the fourth generation hyperbranched polyester and maleic anhydride. A novel cross-linked WHBP/PVA membrane was prepared by adding WHBP into poly(vinyl alcohol) (PVA) solution with glutaraldehyde as the cross-linker. WHBP was characterized by Nuclear Magnetic Resonance and Attenuated Total Reflection Fourier Transform Infrared Spectroscopy (ATR-FTIR), while WHBP/PVA membranes were characterized by ATR-FTIR, X-ray Diffraction, Scanning Electron Microscopy, Thermogravimetric Analysis, mechanical capacity, and water contact angle. Testing results showed that maleic anhydride was grafted on the surface of WHBP; compared with PVA membrane, WHBP/PVA membrane had lower crystallinity, weaker mechanical strength, higher hydrophilicity, and better thermal stability. Sorption and diffusion behaviors of *n*-butanol and water in WHBP/PVA membrane were investigated; pervaporation performances of WHBP/PVA membrane were studied through the dehydration of the 90 wt % *n*-butanol aqueous solution at 40 °C. With an increase of the WHBP content from 0 to 30 wt %, both *n*-butanol uptake and *n*-butanol diffusion coefficient first decreased then increased; *n*-butanol flux first decreased from 10 to 2 $g \cdot m^{-2} \cdot h^{-1}$ then increased to 213 $g \cdot m^{-2} \cdot h^{-1}$; both sorption selectivity and diffusion selectivity first increased then decreased; separation factor first increased from 88 to 1309 then decreased to 16. © 2016 Wiley Periodicals, Inc. J. Appl. Polym. Sci. **2016**, *133*, 43533.

KEYWORDS: composites; cross-linking; membranes; separation techniques; structure–property relations

Received 20 October 2015; accepted 12 February 2016

DOI: 10.1002/app.43533

INTRODUCTION

Pervaporation (PV) is acknowledged as a well-established membrane separation technology with high efficiency and low energy consumption for its applications of the separation and purification of liquid mixtures, extraordinarily in the following three areas: dehydration of organic solvents,[1] recovery of organics,[2,3] and separation of organic–organic mixtures.[4] Different from the conventional distillation where the separation depends on the vapor–liquid equilibrium of the components, pervaporation depends on the sorption–diffusion differences of the feed components in the polymeric membrane. Consequently, the selection and preparation of excellent separation membrane become crucially important in the pervaporation process. To obtain good pervaporation performances for dehydration of organic solvents (alcohols, acids, ethers, ketones, etc.), the membrane should have high affinity and selectivity to water. Various hydrophilic membrane materials with excellent performances for the PV separation of aqueous organic solution such as PVA, chitosan, polysulfone, polyimide, polyamides, and polyaniline[5–13] have been developed and used. Because of its good performances in film forming, hydrophilicity, and chemical-resistant properties, PVA membrane has been applied in the fields of enzyme immobilization, gas separation, fuel cells, and pervaporation dehydration of organics.[7–10] However, because of the semi-crystalline character of PVA, the pervaporation performances of PVA membrane for organics dehydration are not satisfied. It has been demonstrated that the pervaporation properties of PVA membrane could be improved by its modification such as chemical cross-linking, polymer blending and organic–inorganic hybridization.[11] Rachipudi *et al.*[12] developed the sulfonated-PVA membrane using sulfophthalic acid (SPTA) as a cross-linker. Using the membrane to separate water–isopropanol mixtures by pervaporation, the sulfonated-PVA membrane

exhibited preferential selectivity towards water and could be used effectively to separate the water-–sopropanol mixtures. Sridhar *et al.*[13] prepared the nylon 66 blended PVA membrane which cross-linked with glutaraldehyde (GA). The membranes were found to possess good potential for the dehydrating of 2-butanol.

With the progress of polymer science, there has been such an upsurge in the applications of hyperbranched polymers as structural material and nanomaterial, while few attempts have been made for their potential applications in membrane materials. Considering the high reactivity and the highly branched three-dimensional spherical structure of hyperbranched polyester (HBPE), it should be promising to explore the possibility of HBPE as the candidate of membrane material. Moreover, HBPE possesses apparent advantages over linear polymers, for instance, a variety of functional groups, low flexibility, large free-volume, small rheological volume and high solubility in various solvents.[14–17] Wei *et al.*[18] synthetized the hyperbranched poly (amine-ester) (HPAE) and prepared cross-linked HPAE membrane using glutaraldehyde (GA) as the cross-linker, and discussed its pervaporation properties in separating water/isopropanol mixtures. The cross-linked HPAE membranes presented preferable hydrophilicity and high selectivity towards water. Luo *et al.*[19] studied the ethyl cellulose (EC) membrane which was cross-linked by hyperbranched-polyester acrylate (AHBPE) and investigated its PV performance for the separation of benzene/cyclohexane mixtures. Study results indicated that the EC-AHBPE membranes exhibited pre-eminent flux and separation factor.

In this work, a fourth generation of hydroxyl-terminated HBPE was synthesized through the pseudo one-step esterification reaction of 2, 2-bis (hydroxymethyl) propionic acid and 1,1,1-trimethylol propane. But the synthesized HBPE was too insoluble in water, which made it difficult to prepare HBPE-PVA membrane casting solution using water as solvent. Hence, water-soluble hyperbranched polyester (WHBP) was synthesized through the modification of HBPE using maleic anhydride by esterification reaction and characterized by Attenuated Total Reflection Fourier Transform Infrared Spectroscopy (ATR-FTIR) and Nuclear Magnetic Resonance (NMR). Further, novel cross-linked PVA membranes were prepared by incorporating WHBP into PVA solution and used GA as cross-linker. The physic-chemical properties of the resulting WHBP/PVA membranes were characterized by ATR-FTIR, X-ray Diffraction (XRD), Thermogravimetric Analysis (TGA), Scanning Electron Microscopy (SEM), water contact angle and mechanical strength. The effects of WHBP content in PVA membranes on PV performances for the separation of water/*n*-butanol mixtures were studied. Meantime, the sorption–diffusion behaviors of *n*-butanol and water in the WHBP/PVA polymers were also investigated.

EXPERIMENTAL

Materials

Porous ultrafiltration membranes of polyacrylonitrile (PAN) (cutoff MW 5×10^4) were supplied by the Development Center of Water Treatment Technology (China). PVA (average molecular weight approximately 128,000; polymerization degree: 1750 ± 50; hydrolysis degree: 97%), pentaerythritol (PEL), p-toluene sulfonic acid (p-TSA), and 50% glutaraldehyde (GA) solution in water were purchased from GuangFu Institute of Fine Chemicals (Tianjin, China). 2, 2-bis (hydroxymethyl) propionic acid (bis-MPA) was supplied by Aladdin Industrial (Shanghai, China). Maleic anhydride (MA), *n*-butanol and Sulfuric acid (98 wt %) were purchased from Beijing Chemical Works (Beijing, China). Other reagents were of analytical grade and were used without further purification. Home-made deionized water was used throughout the study.

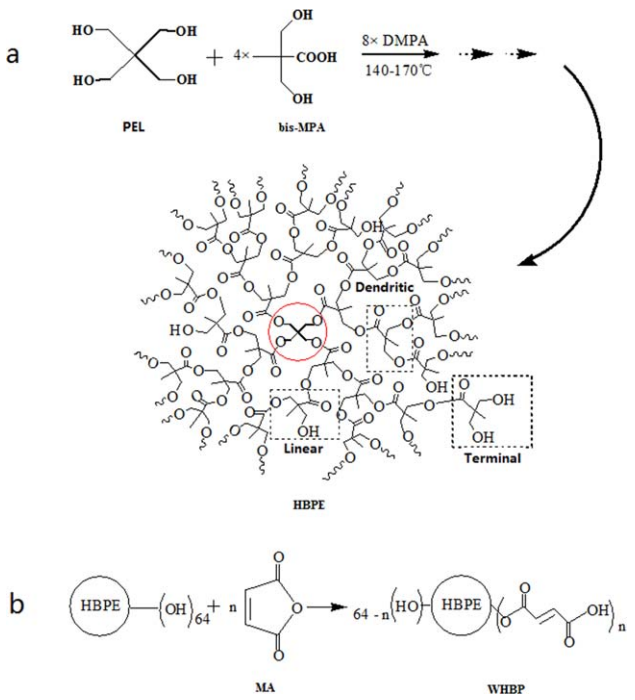

Figure 1. (a) Molecular structure of HBPE and (b) schematic description of the synthesis for WHBP. [Color figure can be viewed in the online issue, which is available at wileyonlinelibrary.com.]

Synthesis of WHBP Polymer

The fourth generation HBPE was synthesized by the melting polycondensation approach in a stepwise manner: with the aid of p-TSA as the catalysis, PEL molecules reacted with bis-MPA which contains one carboxyl (A = COOH) and two hydroxyl (B = OH) functional groups and was recognized as the AB_2 monomer. The synthesis was conducted in a four-necked flask equipped with a nitrogen inlet, a drying tube, and a stirrer at 140–170 °C. The chosen molar ratio of PEL:bis-MPA of 1:60 corresponded to the theoretical molecular weight of HBPE of 7103 g/mol. The synthesized HBPE contains 64 terminal hydroxyl groups as shown in Figure 1(a).

The WHBP can be obtained through the reaction of HBPE and maleic anhydride (MA) according to the literature report.[20,21] The precalculated amount of HBPE and MA were placed in a four-necked flask equipped with a magnetic stirring, a reflux condenser and a nitrogen input. The reaction was carried out at 90 °C and acid titration was conducted to indicate the extent of reaction by 0.1 *M* NaOH methanol solution. The schematic description of the modification process is shown in Figure 1(b).

Membrane Preparation

WHBP/PVA membranes were prepared by solution casting method. A mixture of a certain amount of WHBP, 5 g PVA and 95 mL deionized water was heated for 4 h at 90 °C under stirring; the solution then was filtered to remove bubbles and non-dissolved PVA particles. To make the WHBP/PVA solution cross-linked, 0.25 g cross-linking agent (50% GA water solution) was gradually added under stirring at 250 rpm and pH value 2 (maintained by sulfuric acid). The cross-linked solution was then casted onto the surface of a polyacrylonitrile (PAN) ultrafiltration membrane using a casting knife with a gap of 100 μm and then to be dried in the sterile room at room temperature for 48 hours. Dried at 100 °C under vacuum for 1 h, the membrane was prepared and was ready for PV study. The membranes were designated as M-1, M-2, M-3, M-4, and M-5 corresponding to the mass percentage of WHBP in the membranes which were 0, 5%, 10%, 20%, and 30%, respectively. The overall thickness of the membrane was about 230 μm measured by a micrometer. A total of five measurements of different locations of the membrane surface were tested and were averaged. In addition, to study the effects of the physicochemical properties of the mixed membranes, unmixed and mixed WHBP membranes without support were also prepared. The thickness of the membrane without support was about 60 μm measured by a micrometer (0–150 mm, Shanghai constant measuring tool Co., Ltd).

Membrane Characterization

Nuclear Magnetic Resonance. The ^{13}C NMR spectra of HBPE and WHBP were conducted on an Avance III 400 MHz spectrometer (Bruker, Switzerland) using DMSO-d6 as solvent.

Attenuated Total Reflection Fourier Transform Infrared Spectroscopy. The chemical structure of WHBP and WHBP/PVA membranes were monitored by a Nicolet iS10 ATR-FTIR spectroscope (Thermo scientific, USA) with a resolution of 2 cm and the spectra of 500–4000 cm^{-1}. A small piece of the membrane was pressed against an ATR crystal.

X-ray Diffraction. The crystallinity of the WHBP/PVA membranes was investigated at room temperature by an X-ray diffractometer (D/max-2200-pc, Rigaku, Japan). The diffractograms were measured at a scanning speed of 5°/min in a 2θ range of 5–40° at the tube voltage of 40 kV and the tube current of 20 mA.

Scanning Electron Microscopy. The surface morphology of WHBP/PVA membranes was observed by a scanning electron microscope (JSM-5600LV, JEOL, Japan). Membrane samples were frozen in liquid nitrogen and then were broken to obtain cross-section, sputtered with gold by a Sputter Coater (KYKY SBC-12), the samples then were tested by SEM.

Mechanical Properties. The Mechanical strength of WHBP/PVA membranes was investigated by an Instron 3365 (USA) tensiometer. The shape of the specimens was dumbbell, the length was 30.00 mm, the thickness was 0.10 mm and the width was 4.00 mm. The stretching rate was 50.00 mm/min and each specimen was gauged three to five times to get the average result.

Thermogravimetric Analysis (TGA). Thermal stability of WHBP/PVA membranes was investigated using a thermogravimetric analyzer (SDT Q600, TA Instruments, USA) in a nitrogen atmosphere. The sample was heated from 50 °C to 550 °C with a ramping rate of 10 °C/min.

Static Contact Angle. Water contact angle between water and WHBP/PVA membrane surface was measured with a contact angle meter DSA30 (KRüss GmbH, Germany) at room temperature using the static sessile drop method. Deionized water droplets were dropped onto the membrane surface at five different locations of the same sample to take the average result.

The Total Fractional Free Volume. The total fractional free volume (FFV) was calculated by comparing the theoretical and experimentally measured densities as follows[23]:

$$\text{Total } FFV = FFV_{\text{PVA}} + \frac{(1/\rho_p)\text{-}(1/\rho_{\text{theory}})}{1/\rho_{\text{theory}}} \quad (1)$$

The actual membrane density (ρ_p) can be calculated using

$$\rho_p = \frac{m_{\text{composite}}}{Al} \quad (2)$$

Considering the relevant density, membrane theoretical density (ρ_{theory}) can be calculated using

$$\frac{m_{\text{composite}}}{\rho_{\text{theory}}} = \frac{m_{\text{WHBP}}}{\rho_{\text{WHBP}}} + \frac{m_{\text{PVA}}}{\rho_{\text{PVA}}} \quad (3)$$

The density of the pure WHBP (ρ_{WHBP}) can be calculated using

$$\rho_{\text{WHBP}} = \frac{m_{\text{WSAMPLE}}}{V_{\text{WHBP}}} \quad (4)$$

where m is the mass (g), A is effective membrane area (m^2), l is initial thickness of membrane (m), V_{WHBP} is volume of pure WHBP, m_{WSAMPLE} is the mass of pure WHBP, ρ_{PVA} is 1.27 × 10^3 kg/m^3, which is the density of PVA, FFV_{PVA} was 1.70%.[24]

Swelling Experiments

Membrane swelling experiment can help to understand the interactions between the membrane and the liquid penetrants. The cross-linked WHBP/PVA membranes were dried at 80 °C under vacuum for 48 h and were weighted using a digital microbalance (ACCULAB ALC-110.4, Germany, sensitivity ±0.1 mg). The samples then were immersed in the 90 wt % *n*-butanol/water mixture, pure *n*-butanol or pure water at 40 °C for 24 h to achieve sorption equilibrium. Wiped with filter paper, the swollen membranes were weighted as quickly as possible.[22] Each sample was tested at least three times to get the average result. The degree of swelling (W_∞) was calculated from the following equation:

$$W_\infty = \frac{M_\infty - M_0}{M_0} \quad (5)$$

where M_∞ and M_0 are the masses of the swollen and dry membranes, respectively.

The ideal sorption selectivity α_s was calculated by

$$\alpha_s = W_{W,\infty} / W_{B,\infty} \quad (6)$$

where $W_{W,\infty}$ and $W_{B,\infty}$ are the swelling degrees of the pure water and pure *n*-butanol in the membranes, respectively.[6]

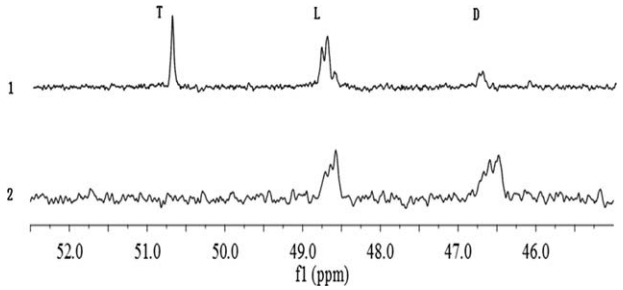

Figure 2. Region of the ^{13}C NMR spectra of HBPE (1) and WHBP (2).

Based on Fick's first and second laws, the diffusion coefficient (D) is a key transport property of solvent molecules in the polymer bulk, and can be defined by the following formula[25]:

$$\frac{M_t}{M_\infty} = \frac{4}{l}\sqrt{\frac{Dt}{\pi}} \tag{7}$$

where M_t is the mass of sorbed solvent at random time t, l is initial thickness of membrane. The Fickian diffusion coefficient can be calculated from the slope of a plot of M_t/M_∞ vs. time $t_{1/2}$. The diffusion selectivity (α_D) was calculated by

$$\alpha_D = D_W / D_B \tag{8}$$

where D_W and D_B are the pure water and pure n-butanol diffusion coefficients, respectively.[26]

Pervaporation Experiments

The pervaporation apparatus used in this work is similar to that reported in our previous article.[27] The feed mixture (40 °C, 90 wt % n-butanol solution) was circulated by a peristaltic pump with a flow rate of 50 L/h, the effective area of the membrane was 28.26 cm^2 and the capacity of the feed compartment was 2000 cm^3. The downstream pressure of the membrane cell was maintained at 80 KPa by a vacuum pump (ZVY-1-10, Shanghai vacdo Vacuum Equipment). When the system reached steady state, at least 2 h after started, the permeate was collected in a cold trap which was immersed in liquid nitrogen, the cold trap with permeate then was weighted lately. Composition of permeate was measured by a gas chromatograph (GC-2014c, Shimadzu, Japan). Membrane PV performances were determined by permeation flux (J), separation factor (α), and PV separation index (PSI). These factors were calculated from the following equations:

$$J = \frac{W}{\Delta t \times A} \tag{9}$$

$$\alpha = \frac{Y_W / Y_B}{X_W / X_B} \tag{10}$$

$$PSI = (\alpha - 1)J \tag{11}$$

where W is the weight of permeate (g); A is the effective membrane area (m^2); Δt is permeation time (h); X_W, Y_W are the mass fractions of water in the feed and in the permeate, and X_B, Y_B are the mass fractions of n-butanol in the feed and in the permeate, respectively.

RESULTS AND DISCUSSION

Membrane Characterization

NMR Studies. From Figure 2, the difference between the ^{13}C NMR spectrum of HBPE and the ^{13}C NMR spectrum of WHBP confirmed that HBPE and WHBP have different chemical structures. For HBPE, the signals at 50.74, 48.80, and 46.73 ppm should be attributed to the quaternary carbon of terminal (T), linear (L), and dendritic (D) fractions, respectively.[14] But for WHBP, the peak intensity of terminal unit almost disappeared while the peak intensities of linear unit and dendritic unit increased. The reason is that hydroxyl groups of the terminal unit of HBPE reacted with MA by esterification reaction as shown in Figure 1(b). When one hydroxy group of the terminal unit in HBPE reacts with MA, a new linear unit will yield. If two hydroxyl groups of the terminal unit reacted with MA, the terminal unit in HBPE would become a new dendritic unit in WHBP.

ATR-FTIR Analysis. Figure 3 shows the ATR-FTIR spectra of the prepared HBPE and WHBP. The strong absorption band in the range 3250–3750 cm^{-1} for -OH indicates the presence of large numbers of hydroxyl groups on the surface of both the HBPE and WHBP, but the decrease of the peak intensity in WHBP has demonstrated the reaction of the terminal hydroxyl. Meanwhile the new absorption peak located at 1641 cm^{-1} for WHBP showed that C = C in MA had been induced into WHBP[14,16] which means that maleic anhydride has been grafted onto the surface of WHBP, which agrees with the results of ^{13}C NMR spectra.

Figure 4 illustrates the ATR-FTIR spectra of the pristine PVA membrane (M-1) and WHBP/PVA membranes (M-2 to M-5). For all membranes, the distinct adsorption bands in the range of 3000–3600 cm^{-1} and at 2925 cm^{-1} correspond to the stretching vibrations of O-H and the asymmetric stretching of C-H, respectively.[28] The intensity of these bands increased significantly as WHBP increased. For WHBP/PVA membranes, the peaks at around 1722 cm^{-1} are attributed to the stretching vibration of C = O in WHBP according to Figure 4. For PVA membrane, the peak at 1650 cm^{-1} corresponds to the stretching

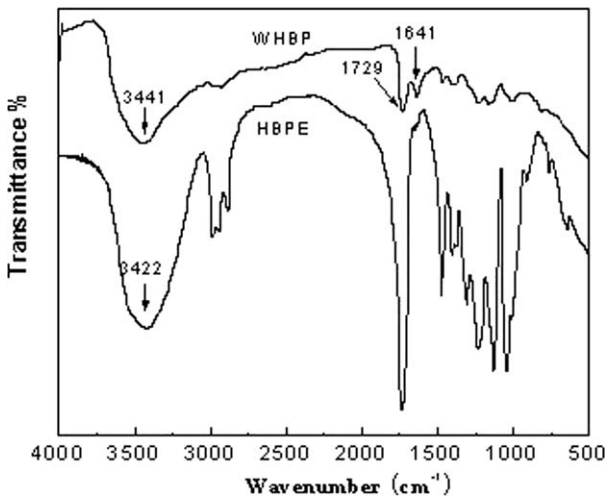

Figure 3. ATR-FTIR spectra of HBPE and WHBP.

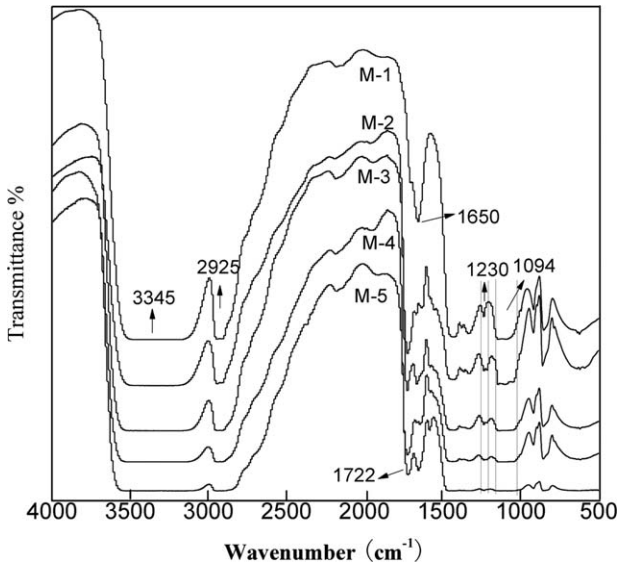

Figure 4. ATR-FTIR spectra of the WHBP/PVA membranes (M-1 to M-5).

of C = O group of the unreacted GA.[13] When WHBP was added into PVA, the intensity of the peaks decreased, which meant that the cross-linking reaction between WHBP and GA occurred by acetalation reaction. Meanwhile, the width of the peaks at 1094 and 1230 cm^{-1} increased significantly, which attributed to C-O and C-O-C groups, which indicated that the acetalation reaction occurred between WHBP-OH and GA-CHO and also, between PVA-OH and GA-CHO.[29] This proved that the added WHBP changed the structure of PVA membrane and the cross-linking reaction occurred between WHBP and glutaraldehyde.

XRD Studies. To study the effect of WHBP on membrane morphology, X-ray diffraction patterns were employed (Figure 5). The pure PVA membrane (M-1) exhibits a typical peak at $2\theta = 20°$, which assigned to the mixture of (101) and (200) crystalline planes.[30,31] For the cross-linked PVA/WHBPE membranes (M-2, M-3, M-4, and M-5), as the content of WHBP increased, the intensity of peak decreased gradually. The reason is that WHBP cross-linked with PVA, as described in ATR-FTIR analysis, which disturbed the ordered packing of PVA polymeric chains and increased the amorphous domains of the cross-linked WHBP/PVA membranes. This structure caused the increase of membrane free volume, which was good for the diffusion of permeate molecules, and as a result, permeation flux increased.

SEM Studies. The morphology of the top surfaces of the PVA and WHBP/PVA membranes for M-1 to M-5 and cross-sectional morphology of M-5 was observed with scanning electron microscopy (SEM) (Figure 6). With an increase of WHBP content from 0 to 30 wt %, membrane surfaces changed from smooth to rough. The surfaces of M-1 and M-2 were smooth and dense with no appreciable voids. There were some holes on the surface of M-3 which were caused by the air bubbles in casting solution because of the stir. When WHBP content increased to 30 wt % (M-5), phase separation between PVA and WHBP occurred, the nonselective defect voids formed and WHBP particles appeared on the membrane surfaces. This was because the unreacted WHBP precipitated on membrane surface.

Mechanical Properties. Membrane mechanical properties were evaluated by the tensile strength and elongation at break as shown in Figure 7. PVA membrane shows a high tensile strength because of its high crystallinity. With the increase of WHBP content, both tensile strength and the elongation at break decreased quickly. A similar situation was observed by Singha *et al.*[11] who prepared the modified PVA membrane by the cross-linking copolymerization of acrylic acid and hydroxyethylmethacrylate. For the decrease of the tensile strength, it may be because that, with the increase of WHBP, membrane crystallinity decreased and caused the increase of membrane free-volume as described in the section XRD Studies. For the decrease of elongation at break, it may because, with the increase of WHBP, chain flexibility of the polymer reduced for the reason of the cross-linking of the spherical WHBP molecules and the linear PVA molecules.[12]

TGA Studies. The thermal stability of PVA membrane (M-1) and WHBP/PVA membranes (M-2 to M-5) was investigated through the thermo-gravimetric analysis (Figure 8). For all membranes, when the temperature increased from 50 °C to 200 °C, the weight of the membranes only reduced slightly for the reason of vaporization of the absorbed water in membranes. The weight loss at 210–360 °C was ascribed to the degradation of the main polymer chain.[6,12] Because of the carbonation of polymer matrix, more than 90% weight was lost before 480 °C and the membranes decomposed completely at around 500 °C. From Figure 8, the PVA membrane started to degrade at 210 °C, while the WHBP/PVA membranes started to decompose at 300 °C, and the decomposition temperature of the WHBP/PVA membranes increased with the increase of WHBP content, which indicated that the thermal stability of the WHBP/PVA membranes could be enhanced by the adding of WHBP. This

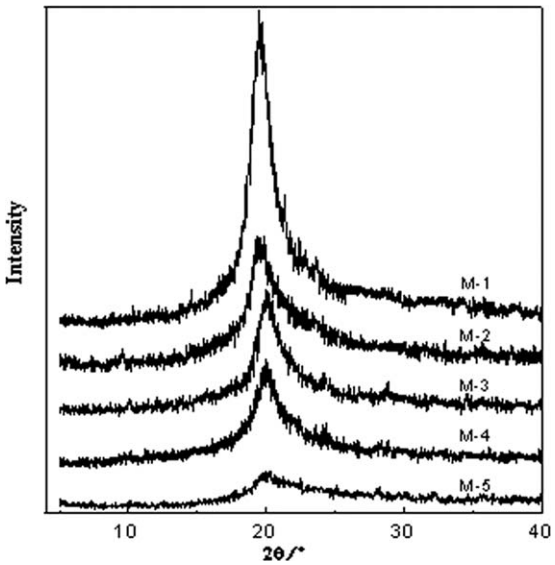

Figure 5. XRD patterns of the membrane of M-1 to M-5.

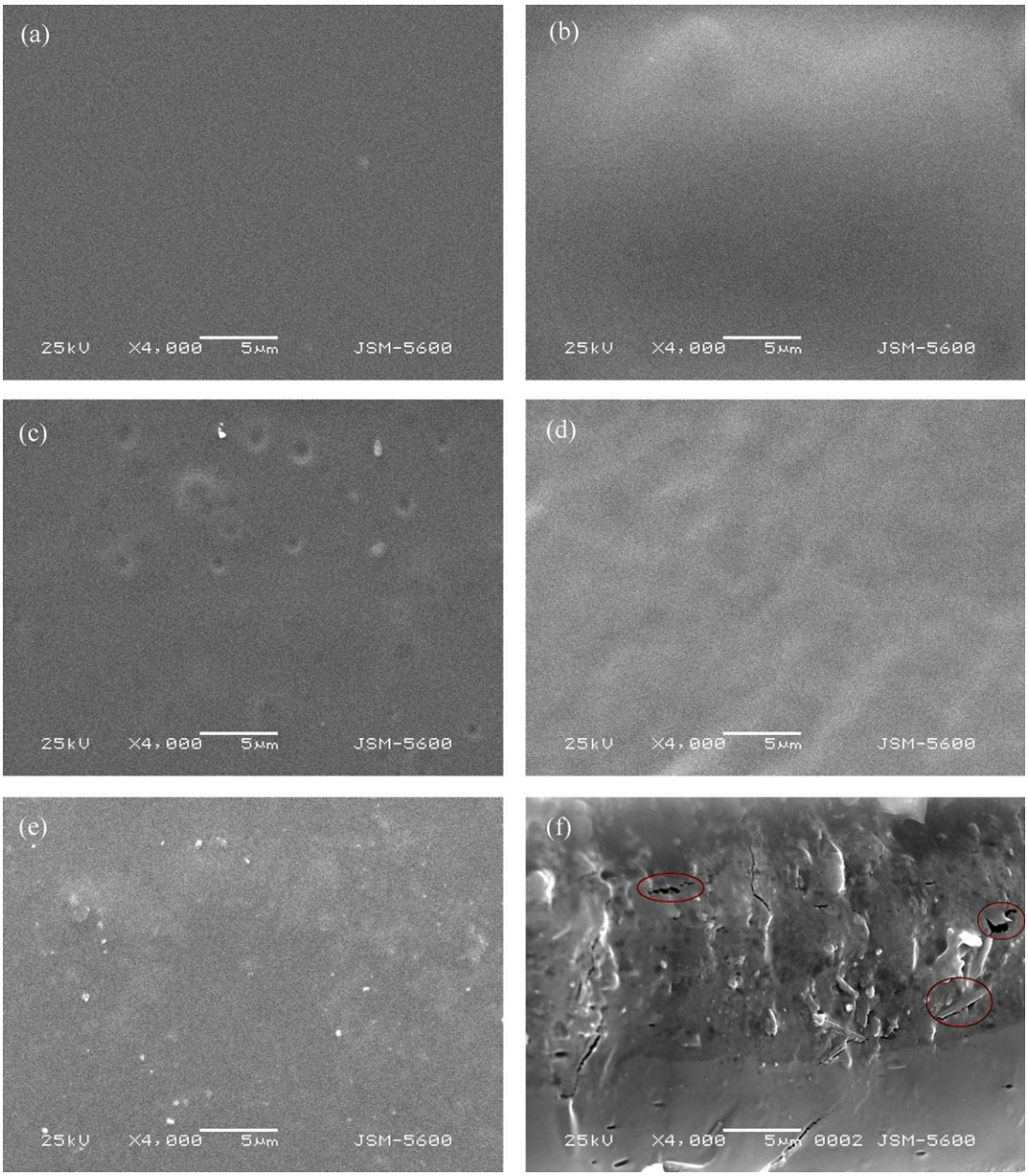

Figure 6. SEM images of the top surfaces of (a) M-1, (b) M-2, (c) M-3, (d) M-4, (e) M-5, and (f) the cross-sectional image of M-5. [Color figure can be viewed in the online issue, which is available at wileyonlinelibrary.com.]

was attributed to the nature of the membrane cross-linking network as analyzed in membrane ATR-FTIR studies.

Water Contact Angle Studies. Contact angle is widely used in membrane material science to describe the hydrophilicity of a membrane surface. Contact angle determines wetting and adhesion behavior of the surface, so the contact angle between water and membrane surface is important for the understanding of transport process. Contact angle between water and membrane surface was measured and was shown in Figure 9. Compared with the WHBP/PVA membranes, pure PVA membrane has the highest contact angle (58°) and with the increasing of WHBP content in the membrane matrix from 0% to 30%, water contact angle decreased quickly from 58° to 20°. This was because there are a large number of hydroxyl groups and carboxyl groups in WHBP as shown in Figure 1. This indicated that water molecules are easily dissolved in the WHBP/PVA membranes, which means adding WHBP to the membrane matrix could increase membrane hydrophilicity and then improve its pervaporation performance.[32]

Total FFV Studies. In order to study the effect of WHBP on the microstructure of membrane, it is important to know the total FFV of the adding WHBP which can fundamentally change the diffusion of the molecules through the membranes.[23] To use eq. (2), membrane density measurements were carried out. From Figure 10(a), the increasing of WHBP concentration caused the decrease of membrane density, and the increase of

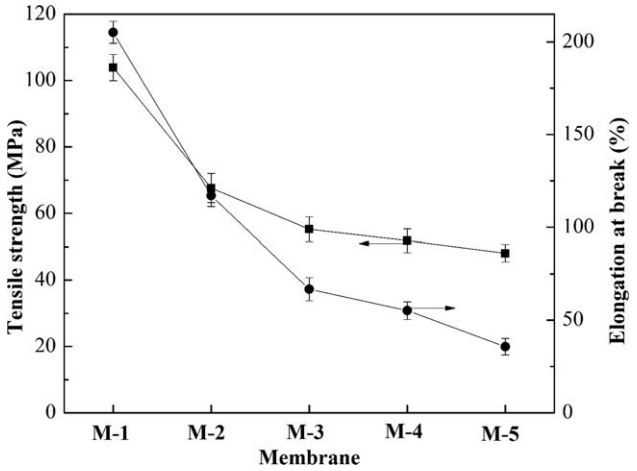

Figure 7. Tensile strength and tensile elongation of PVA and WHBP/PVA membranes.

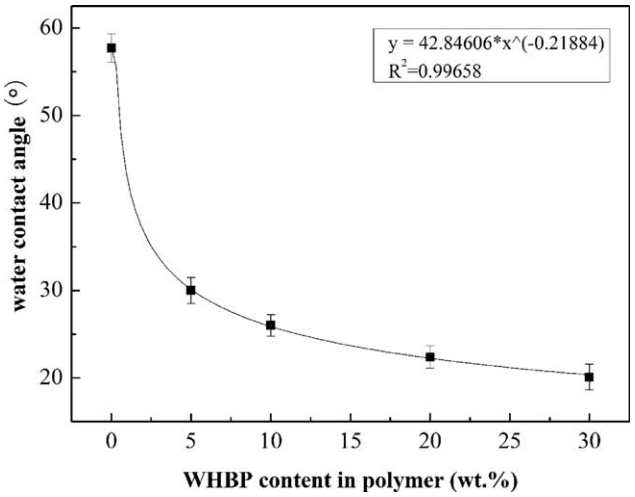

Figure 9. Water contact angle of WHBP/PVA membranes.

the free volume in membrane matrix as shown in Figure 10(b). Consequently, the WHBP/PVA membranes could offer more diffusion paths for those small penetrants.

Swelling Analysis

In PV, membrane swelling behavior controls the transport of penetrants under the influence of chemical gradient. The swelling results can illustrate the interactions between the membranes and the penetrant molecules. In order to study the effects of WHBP content on membrane swelling, swelling degree of various WHBP/PVA membranes in a 90 wt % *n*-butanol/water mixture was plotted in Figure 11. According to XRD, the cross-linking between WHBP and GA decreased the crystallinity of the membranes, as a result, the swelling degree enhanced.[26,33] Conversely, in this study, with the increase of WHBP in the WHBP/PVA membranes, the swelling degree decreased, that is to say the membranes prepared in this method exhibited a good stability in water. It could be explained that the cross-linking of WHBP and GA restricted the mobility of polymer chains. This effect of cross-linking behavior on membrane swelling properties overtook the effect of the decrease in crystallinity on membrane swelling properties. With the addition of WHBP, more and more cross-linking reactions happened as described in ATR-FTIR Analysis, which made the amorphous regions of the PVA membrane network more and more compact,[12] which in turn caused the improvement of the selectivity of the WHBP/PVA membranes.

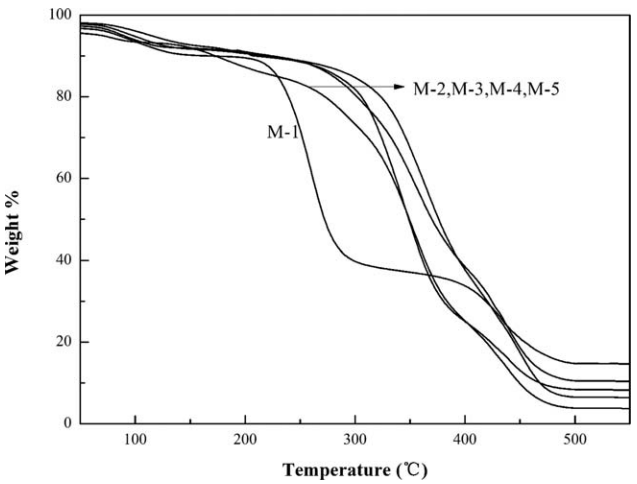

Figure 8. Thermogravimetric curves of PVA membranes with different content of WHBP.

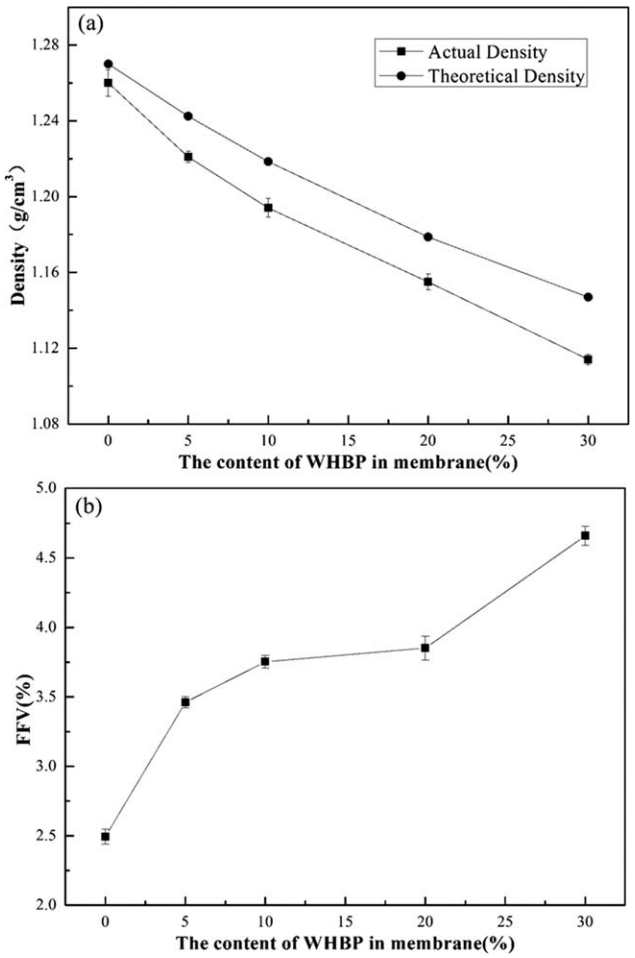

Figure 10. Effects of WHBP content on (a) the density, (b) the FFV of WHBP/PVA membranes.

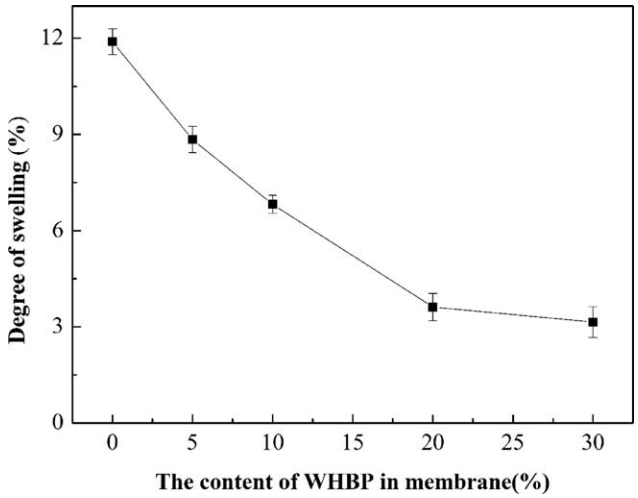

Figure 11. Swelling extent of membranes made from different concentrations of WHBP.

The typical sorption history of the PVA and PVA/WHBP membranes in pure *n*-butanol (a) and water (b) at 40 °C is shown in Figure 12. For all membranes, water sorption was higher than *n*-butanol sorption. When WHBP content increased from 0% to 30%, water uptake increased from 0.74 to 1.27 kg/kg; For *n*-butanol uptake, when WHBP increased from 0% to 20%, it decreased significantly from 0.24 to 0.02 kg/kg; but when WHBP further increased from 20% to 30%, it increased from 0.02 to 0.04 kg/kg. So as shown in Figure 13(b), with the increase of WHBP from 0% to 30%, the sorption selectivity firstly increased from 2.96 to 58.07 then decreased to 31.84. This can be interpreted that, with the increase of WHBP, the hydrophilicity of the membrane increased as analyzed in the section Water Contact Angle Studies, but when WHBP increased to 30%, the phase separation between PVA and WHBP appeared as shown in Figure 6 and caused the aggregation of the WHBP which in turn resulted in the nonselective defects voids on the membranes, so the sorption selectivity decreased.[27]

Diffusion coefficients of *n*-butanol and water in the WHBP/PVA membranes are presented in Figure 13(a). The diffusion rate of water was two orders of magnitude faster than that of the *n*-butanol. With an increase of WHBP addition, the diffusion coefficient of water increased and the diffusion coefficient of *n*-butanol firstly decreased then lightly increased. According to eq. (8), the diffusion selectivity of water/*n*-butanol firstly increased then decreased as shown in Figure 13(b). With the increase of WHBP content in PVA membranes, the free volume in the membrane matrix increases as shown in Figure 10(b), so permeate diffusion coefficient increases[34]; meanwhile, the cross-linking reaction between WHBP and GA (shown in ATR-FTIR Analysis) made the PVA membrane network more compact[12]; moreover, because of water molecular is smaller than that of the *n*-butanol molecular, more and more water molecules and less and less *n*-butanol molecules penetrated through the WHBP/PVA membranes, so the diffusion selectivity increased.[32,33] But when WHBP addition increased to 30%, the nonselective defect voids formed in membrane [as shown in Figure 6(f)] and resulted the increase of the diffusion of *n*-butanol molecules [as shown in Figure 13(a)] and the decrease of diffusion selectivity.[26]

Pervaporation Properties

To examine the pervaporation performances of the PVA and WHBP/PVA membranes, pervaporation experiment for the dehydration of the 90 wt % *n*-butanol/water mixture was carried out at 40 °C and the experiment results were shown in Figure 14. With the increase of WHBP content, both total flux and water flux increased, but *n*-butanol flux firstly decreased and then increased quickly. When WHBP content was smaller than 20 wt %, *n*-butanol flux was negligible small and water flux was very close to the total flux, which means that the tested membranes had a high selectivity toward water. The incorporation of WHBP to the PVA matrix not only increased the hydrophilicity and the free volume of the membranes but also made the mobility of the PVA chains dropped for the reason of the cross-linking of the membrane matrix. With the increase of WHBP content from 0% to 30%, both water uptake and water diffusion coefficient increased; *n*-butanol uptakes and *n*-butanol

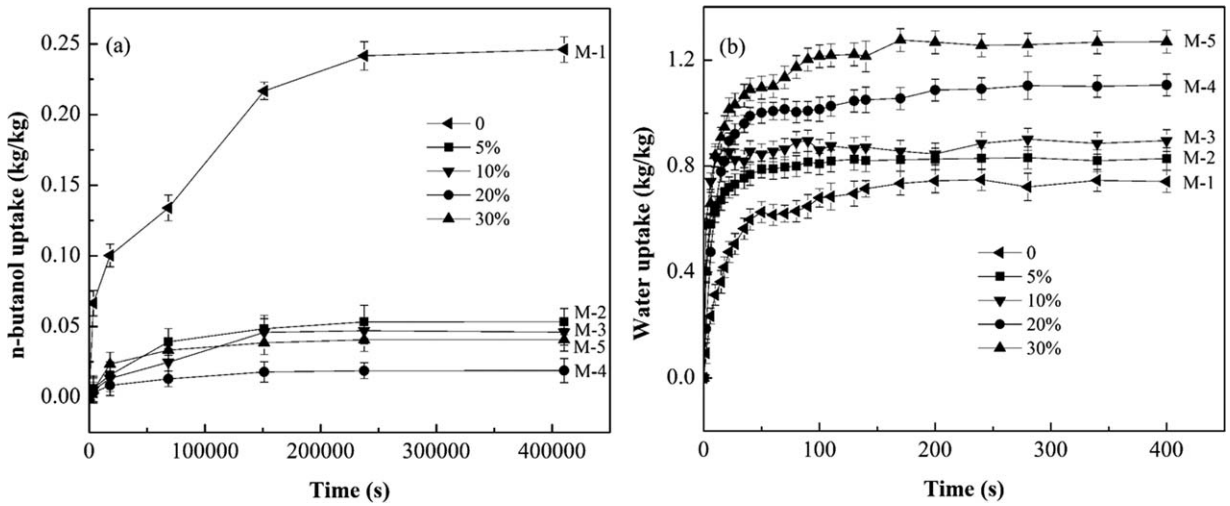

Figure 12. Water and *n*-butanol sorption curves of PVA and PVA/WHBP membranes at 60 °C.

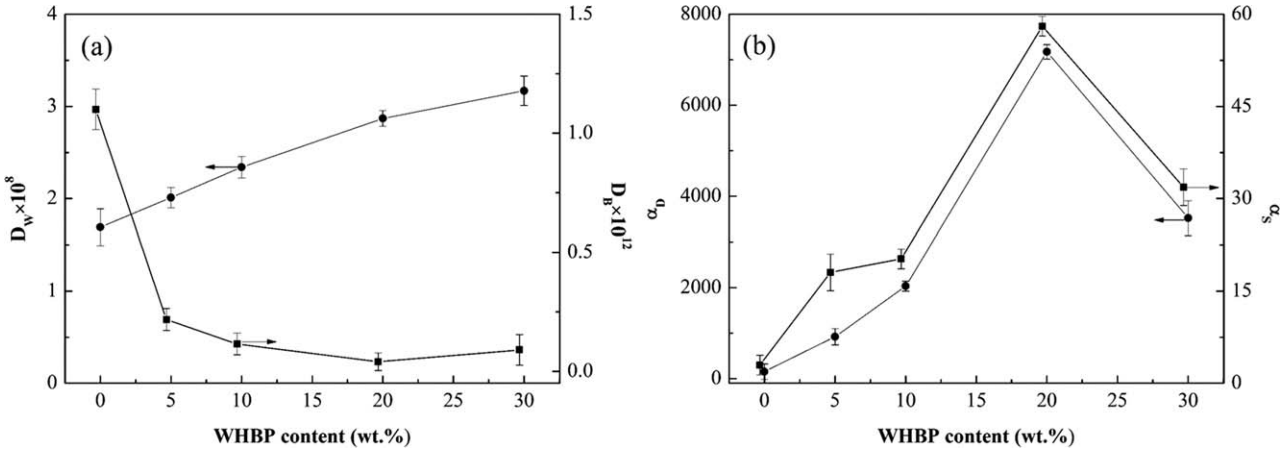

Figure 13. Effects of WHBP content on (a) diffusion coefficients, (b) sorption selectivity and diffusion selectivity of pure *n*-butanol and pure water.

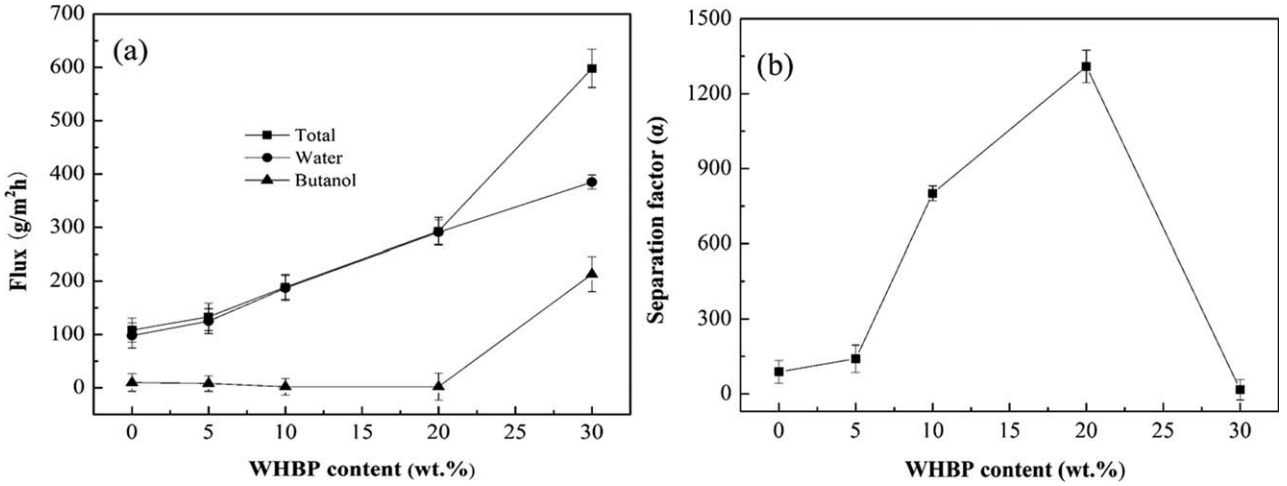

Figure 14. Effects of WHBP content on (a) total flux, partial flux, (b) separation factor.

diffusion coefficient firstly increased and then decreased, as a result, water flux increased from 101 to 385 $g \cdot m^{-2} \cdot h^{-1}$, and *n*-butanol flux firstly decreased from 10 to 2 $g \cdot m^{-2} \cdot h^{-1}$ then increased to 213 $g \cdot m^{-2} \cdot h^{-1}$ quickly. With the increase of WHBP content, separation factor first increased then decreased quickly. As showed in Figure 13(b), with the increase of WHBP content, both the sorption selectivity and the diffusion selectivity first increased then decreased. This is because of the addition of WHBP increased both the hydrophilicity and the free volume of the membranes. While WHBP addition increased to 30%, the phase separation between PVA and WHBP occurred and the nonselective defect voids formed, so we can see that the separation factor first increased then decreased.

PSI is a guideline for the selection of a membrane with an optimal combination of flux and selectivity for industrial pervaporation process. From the plot of Figure 15, with the increase of WHBP in the membrane, *PSI* climbed to the highest value when WHBP content was 20 wt % and then dropped dramatically for the reason of the sharp decrease of separation factor. From practical point of view, the membrane M-4 had a good pervaporation performance for the dehydration of the 90 wt % *n*-butanol/water mixture.

CONCLUSIONS

In this article, water-soluble hyperbranched polymer (WHBP) was prepared by the modification of the fourth-generation hyperbranched polyester with maleic anhydride. Then, using the

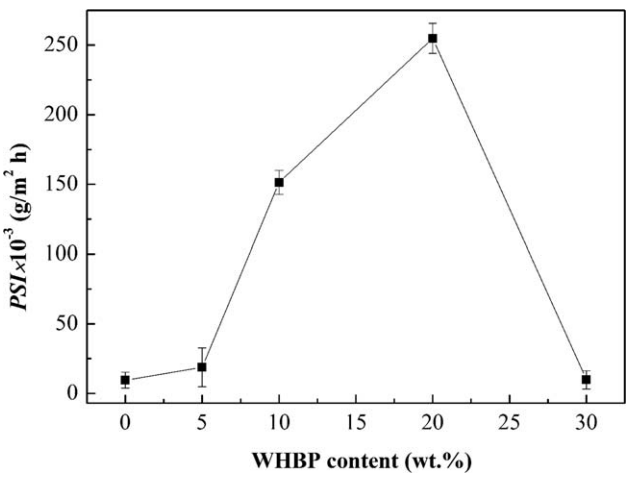

Figure 15. Effects of WHBP content on permeate separate index.

prepared WHBP as a modifier and the glutaraldehyde as a cross-linker, a novel cross-linked WHBP/PVA membrane was produced.

For the WHBP/PVA membranes, with an increase of WHBP, more cross-linking reaction occurred. This made the amorphous region of membrane network more compact, membrane crystallinity decreased, membrane mechanical property of worsened, membrane thermal stability enhanced, and swelling degree decreased. Meanwhile, with the adding of WHBP, both of hydrophilicity and free volume of the membrane increased, so the uptake and the diffusion coefficient of the water increased. As a result, water flux increased from 101 to 385 $g \cdot m^{-2} \cdot h^{-1}$. When WHBP addition was 30%, because of the emerging of the nonselective defect voids in membrane, *n*-butanol flux first decreased from 10 to 2 $g \cdot m^{-2} \cdot h^{-1}$ then increased to 213 $g \cdot m^{-2} \cdot h^{-1}$. Both of sorption selectivity and diffusion selectivity first increased then decreased, and the maximum value was appeared when WHBP was 20%. Accordingly, separation factor firstly increased from 88 to 1309 then decreased to 16. When the WHBP content was 20 wt %, membrane showed the best PV performances with the highest *PSI* of 3.83×10^6 $g \cdot m^{-2} \cdot h^{-1}$.

ACKNOWLEDGMENTS

The authors gratefully acknowledges the financial support from Jilin Provincial Science & Technology Department (No: 20150204077GX), the Foundation of Key Programs for Science and Technology of Changchun (No: 2013058) and Science & Technology Research Program of Changchun University of Technology (No: 2012010).

REFERENCES

1. Chapman, P. D.; Oliveira, T.; Livingston, A. G.; Li, K. *J. Membr. Sci.* **2008**, *318*, 5.
2. Vane, L. M. *J. Chem. Technol. Biotechnol.* **2005**, *80*, 603.
3. Karlsson, H. O. E.; Trägårdh, G. *J. Membr. Sci.* **1993**, *76*, 121.
4. Smitha, B.; Suhanya, D.; Sridhar, S.; Ramakrishna, M. *J. Membr. Sci.* **2004**, *241*, 1.
5. Zhang, Q. G.; Liu, Q. L.; Zhu, A. M.; Xiong, Y.; Ren, L. *J. Membr. Sci.* **2009**, *335*, 68.
6. Tang, Y. P.; Widjojo, N.; Shi, G. M.; Chung, T. S.; Weber, M.; Maletzko, C. *J. Membr. Sci.* **2012**, *415–416*, 686.
7. Wang, Y.; Hsieh, Y. L. *J. Membr. Sci.* **2008**, *309*, 73.
8. Yegani, R.; Hirozawa, H.; Teramoto, M.; Himei, H.; Okada, O.; Takigawa, T.; Ohmura, N.; Matsumiya, N.; Matsuyama, H. *J. Membr. Sci.* **2007**, *291*, 157.
9. Gu, S.; He, G. H.; Wu, X. M.; Guo, Y. J.; Liu, H. J.; Peng, L.; Xiao, G. K. *J. Membr. Sci.* **2008**, *312*, 48.
10. Qiao, X. Y.; Chung, T. S.; Guo, W. F.; Matsuura, T.; Teoh, M. M. *J. Membr. Sci.* **2005**, *252*, 37.
11. Singha, N. R.; Kar, S.; Ray, S.; Ray, S. K. *Chem. Eng. Process.* **2009**, *48*, 1020.
12. Rachipudi, P. S.; Karidurаganavar, M. Y.; Kittur, A. A.; Sajjan, A. M. *J. Membr. Sci.* **2011**, *383*, 224.
13. Sridhar, S.; Smitha, B.; Reddy, A. A. *Colloids Surf A: Physicochem. Eng. Asp.* **2006**, *280*, 95.
14. Wang, X. X.; Lai, G. Q.; Jiang, Z. G.; Zhang, Y. F. *Eur. Polym. J.* **2006**, *42*, 286.
15. Jena, K. K.; Narayan, R.; Raju, K. V. S. N. *J. Appl. Polym. Sci.* **2010**, *118*, 280.
16. Kou, Y. X.; Wan, A. J.; Tong, S. Y.; Wang, L.; Tang, J. W. *React. Funct. Polym.* **2007**, *67*, 955.
17. Gataulina, A. R.; Khannanov, A. A.; Malinovskikh, O. A.; Bondar', O. V.; Ulakhovich, N. A.; Kutyreva, M. P. *Russ. J. Gen. Chem.* **2013**, *83*, 2269.
18. Wei, X. Z.; Liu, X. F.; Zhu, L. P.; Zhu, B. K.; Wei, Y. F.; Xu, Y. Y. *J. Membr. Sci.* **2008**, *307*, 292.
19. Luo, Y. J.; Xin, W.; Li, G. P.; Yang, Y.; Liu, J. R.; Lv, Y.; Jiu, Y. B. *J. Membr. Sci.* **2007**, *303*, 183.
20. Asif, A.; Shi, W. F. *Eur. Polym. J.* **2003**, *39*, 933.
21. Žagar, E.; Žigon, M. *Prog. Polym. Sci.* **2011**, *36*, 53.
22. Xia, L. L.; Li, C. L.; Wang, Y. *J. Membr. Sci.* **2016**, *498*, 263.
23. Nour, M.; Berean, K.; Chrimes, A.; Zoolfakar, A. S.; Latham, K.; McSweeney, C.; Field, M. R.; Sriram, S.; Kalantar-zadeh, K.; Ou, J. Z. *J. Membr. Sci.* **2014**, *470*, 346.
24. Lue, S. J.; Lee, D. T.; Chen, J. Y.; Chiu, C. H.; Hu, C. C.; Jean, Y. C.; Lai, J. Y. *J. Membr. Sci.* **2008**, *325*, 831.
25. Shi, G. M.; Chen, H. M.; Jean, Y. C.; Chung, T. S. *Polymer* **2013**, *54*, 774.
26. Sun, D.; Yang, P.; Li, L.; Yang, H. H.; Li, B. B. *Korean J. Chem. Eng.* **2014**, *10*, 1877.
27. Sun, D.; Li, B. B.; Xu, Z. L. *Desalination* **2013**, *322*, 159.
28. Yuan, H. K.; Ren, J.; Ma, X. H.; Xu, Z. L. *Desalination* **2011**, *280*, 252.
29. Zhang, L.; Yu, P.; Luo, Y. B. *J. Membr. Sci.* **2007**, *306*, 93.
30. Kulkarni, S. S.; Kittur, A. A.; Aralaguppi, M. I.; Karidurаganavar, M. Y. *J. Appl. Polym. Sci.* **2004**, *94*, 1304.
31. Kim, D. S.; Park, H. B.; Rhim, J. W.; Lee, Y. M. *Solid State Ionics* **2005**, *176*, 117.
32. Lin, W. H.; Li, Q.; Zhu, T. R. *J. Ind. Eng. Chem.* **2012**, *18*, 941.
33. Lue, S. J.; Chien, C. F.; Mahesh, K. P. O. *J. Membr. Sci.* **2011**, *384*, 17.
34. Yeang, Q. W.; Zein, S. H. S.; Sulong, A. B.; Tan, S. H. *Sep. Purif. Technol.* **2013**, *107*, 252.